Chemical Influence of Pore Pressure on Brine Flow in Clay-Rich Material

Etienne Cassini[1(✉)], Danila Mylnikov[1], and Roman Makhnenko[1,2]

[1] Laboratory of Soil Mechanics – Chair "Gaz Naturel" Petrosvibri, Swiss Federal Institute of Technology (EPFL), Lausanne, Switzerland
etienne.cassini@epfl.ch
[2] Department of Civil and Environmental Engineering, University of Illinois at Urbana-Champaign, Urbana, USA

Abstract. Hydromechanical properties of shales are complex due to the involved material structure, with the solid matrix being mainly formed by swelling clays and porosity dominated by nanometer scale tortuous voids with large aspect ratios. Intrinsic permeability of restructured Opalinus Clay (Swiss shale) brought to shallow geological storage conditions was measured with *in situ* brine. Under constant temperature, vertical stress, and downstream fluid pressure, steady-state flow experiments show a significant trend of permeability decrease with increasing differential (upstream minus downstream) fluid pressure, thus contradicting the conventional Darcy's description. To interpret these experimental measurements, brine permeability is derived using a one-step self-consistent homogenization scheme based on the knowledge of material's pore structure. While mechanical and thermal effects cannot explain the permeability decrease, the trend is reproduced with the correct order of magnitude by considering a chemical effect: a pore size reduction in the sample due to water adsorption at mineral surface.

Introduction

Shales are fissile rock formations composed of inert mineral inclusions embedded in a clay matrix (Weaver 1988). The amount of clay is usually very high, e.g. around 60% in Opalinus Clay - a Swiss shale (Bossart 2012), and as a consequence shales exhibit certain particular features, such as high level of anisotropy, self-healing capacity, and very low permeability. Because of the high specific surface area of the clay minerals and their *mille-feuille* structure, shale's behavior is also very sensitive to water saturation and its chemical composition. Shales now are broadly considered as seals for nuclear waste and CO_2 storage and in petroleum industry for unconventional gas exploitation. Therefore, fluid and gas permeability, including permeability to *in situ* water or brine, are the key parameters to study for the safety, the efficiency, and the scientific comprehensiveness of the material.

Permeability of a geomaterial is a macro-parameter, which is influenced by the structure of its pore system and eventual chemical phenomenon leading to pore size reduction or pore closure. Permeability measurements provide important information on the material's microstructure, especially in a case where direct investigations at

A. Ferrari and L. Laloui (eds.), *Advances in Laboratory Testing and Modelling of Soils and Shales (ATMSS)*, Springer Series in Geomechanics and Geoengineering,
DOI 10.1007/978-3-319-52773-4_31

the micro-scale are impossible. To conclude on material behavior at micro-level, permeability measurements should demonstrate high level of accuracy and confidence, which can be achieved by the steady-state flow technique. In this paper we discuss the results on permeability measurements for clay-rich material during steady-state flow of brine and interpret them considering water adsorption, with a one-step self-consistent homogenization scheme.

Experimental Methods

Remolded (i.e., reconstituted) shale – Opalinus Clay – saturated with natural brine (Pearson 2002) is studied in the current work. Remolded specimens are prepared by crushing the intact material in a grinder, sieving the particles with a size smaller than 0.5 mm, mixing with brine corresponding to approximately 1.5 times the liquid limit (or 60%), and consolidating at 350 kPa vertical stress for at least 72 h in one-dimensional conditions. Obtained cylindrical specimens have porosity of 0.33 and the degree of saturation is 0.85 – 0.90. Crushing of shale preserves the flake-like structure

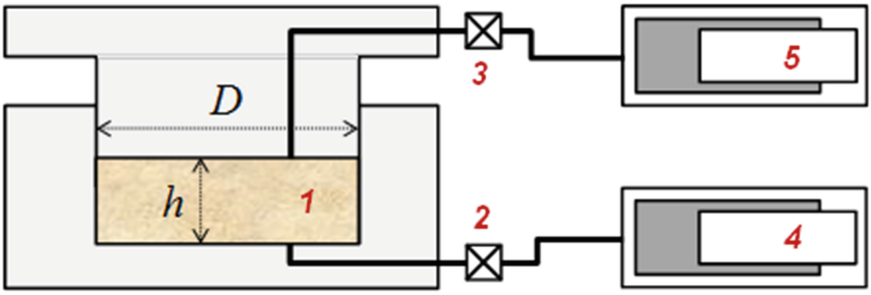

Fig. 1. Scheme of the experimental setup. 1 – rock specimen inside the oedometric cell; 2 and 3 – upstream and downstream pressure transducers respectively; 4 and 5 – upstream and downstream pressure/volume controllers respectively.

of an intact material and eliminates structural anisotropy.

Tested specimen (height h = 12.5 mm and diameter D = 35 mm) is then gradually brought to *in situ* conditions in the oedometric cell: 27 MPa axial total stress (σ_v) and 8 MPa pore pressure (p), which results in the porosity reduction to 0.15. Back pressure saturation method is implemented for 7 days with graduate increase of upstream and downstream pressures and promoting the flow through the specimen. It allows achieving full saturation (at p > 7 MPa) that is confirmed by measurements of constant Skempton's B coefficient values while the effective mean stress (P') is preserved to be the same (ASTM D4767 2011) and equal to 9 MPa. Recorded undrained pore pressure increments are corrected for the influence of "dead" volume (Makhnenko and Labuz 2016) and provide B = 0.85, while B is measured to be isotropic and equal to 0.99 in

conventional triaxial cell at $P' = 0.2$ MPa. Effective mean stress and bulk modulus are calculated from applied vertical stress and vertical deformation by taking drained Poisson's ratio $\nu = 0.3$ (measured in conventional triaxial test at $P' = 0.2 - 0.7$ MPa). Biot coefficient α is calculated from measured unjacketed bulk modulus $K_s' = 8.9$ GPa and the bulk modulus of the brine at pressures above 3 MPa is found to be $K_{br} = 2.0$ GPa – slightly lower than the one of pure water. Summary of the material parameters of

Table 1. Material properties of remolded shale at $\sigma_v = 27$ MPa, $p = 8$ MPa.

Porosity n, [-]	Bulk modulus K, [GPa]	Skempton's coef. B, [-]	Biot coef. α, [-]	Poisson's ratio ν, [-]
0.15	2.5	0.85	0.72	0.3

investigated remolded shale is given in Table 1.

Results

Brine permeability of shale is reported as an intrinsic permeability k_{int} that is determined from Darcy's law after achieving steady-state flow conditions:

$$k_{int} = \frac{4\eta_{br} h \Delta V}{\pi D^2 \Delta p_{diff} \Delta t} \tag{1}$$

Here η_{br} is brine viscosity equal to 0.001 Pa·s, Δp_{diff} is the differential fluid pressure, and ΔV is the fluid volume that passed through the specimen during the time period Δt. The differential fluid pressure is determined as the difference in readings of the upstream and the downstream pressure transducers (Fig. 1). Upstream and downstream pressure/volume controllers provide measurements of brine volume that enters and exits the specimen respectively.

Considering all the contributing factors, permeability is reported with the accuracy of 2.5% when the duration of steady-state flow exceeds 12 h. Steady-state condition and the consistence of the measurements are ensured by obtaining constant permeability values with standard deviation of 2.5% for several consecutive flow cycles at a fixed differential fluid pressure.

Permeability of the material is measured at several differential pressure values after the steady-state flow of brine is established through the specimen. Downstream fluid

Table 2. Values of brine permeability for the remolded shale as a function of differential fluid pressure.

Differential pressure, MPa	1.5	3.0	6.0	8.0
Intrinsic permeability, m^2	1.3e-20	1.2e-20	9.0e-21	8.5e-21

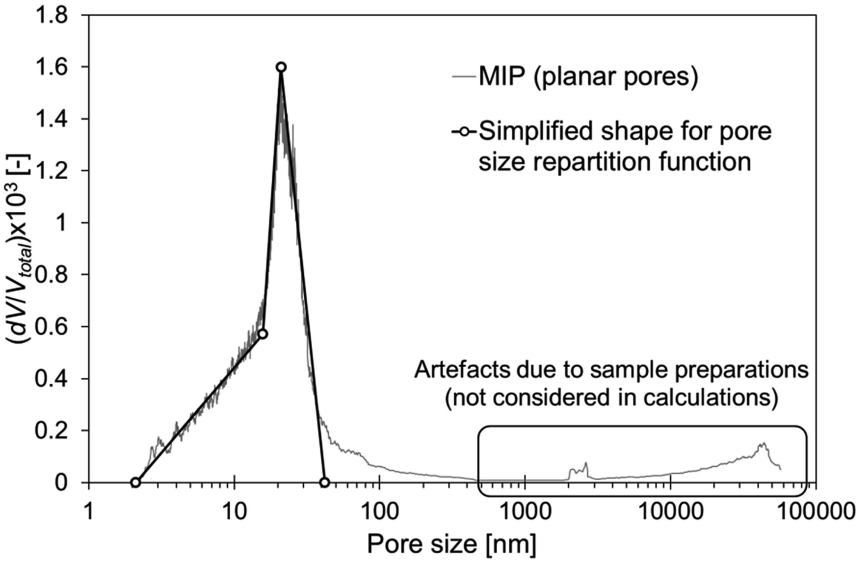

Fig. 2. MIP measurements of pore size distribution in tested remolded shale with hypotheses of planar pores (V - volume of intruded mercury).

pressure is kept at constant value of 8 MPa, while upstream pressure is increased several times. The results demonstrate consistent nonlinear decreasing trend of brine permeability with increasing differential fluid pressure (Table 2).

Measured values of remolded shale (Opalinus Clay) permeability are $\sim 10^{-20}$ m^2, while reported intrinsic permeability of the intact material ranges from 10^{-21} to 10^{-19} m^2 (Romero et al. 2013). Mercury intrusion porosimetry (MIP) measurements performed on the tested sample show a mono-modal pore size repartition with a peak at 21 nm inter-platelet distance (Fig. 2). Pores of this size are supposed to be flat (crack-like) and localized in the clay matrix.

Discussion

Observed decreasing trend of intrinsic brine permeability of remolded shale, with increasing fluid differential pressure at constant downstream pressure, cannot be explained using only the poromechanical considerations. An increase in brine pressure upstream with constant downstream pressure should lead to increase in both porosity and pores size upstream and preserve the microstructure downstream, leading to a global increase of the permeability. Moreover, this increase in porosity and permeability is evaluated using poroelastic relationships to be on the order of a few percent, whereas the decrease in permeability observed here is of 35%. Also, the observed trend cannot be explained by a thermal effect, e.g., for a conservative calculation that

considers unidirectional flow between two adiabatic platelets. Using Stokes equations for non-isotherm viscous flow and brine thermal conduction at 24 °C of 0.6 $W{\cdot}m^{-1}{\cdot}K^{-1}$, the elevation of temperature along the flow can be shown to be much lower than 1 °C.

Suggested explanation of the experimental observations deals with chemistry and a reduction of the brine accessible porosity in the upstream section of the sample where brine pressure is higher. Due to the characteristic structure of shale, with very small pores and high specific surface area, brine adsorption at the clay surface, which increases with fluid pressure, should be considered. The thickness of a single layer of water is of 0.3 nm, so the adsorption of multiple water layers at the surface of clay minerals in the shale sample can lead to the closure of the smallest pores ($\sim$ nm) and cause a reduction of the effective pore size of the larger pores.

In this work, a numerical derivation of the sample permeability, assumed to be isotropic, is performed based on continuum fluid mechanics and homogenization theory (Dormieux et al. 2006). The goal of the modeling is to investigate if water adsorption is a good candidate for explaining the experimental data, both in terms of the trend and the order of magnitude. The simulation is based on a decomposition of the sample in 20 vertical layers where pressure is supposed to be constant. The permeability of each layer is calculated iteratively from upstream to downstream to determine the brine pressure in the next layer and then deduce its permeability. Flow is constant between the different layers and the convergence criterion is on the downstream pressure. Calculations are performed in MatLab©.

Based on continuum fluid mechanics considerations at the nanoscale and a slipping boundary condition between brine and mineral surface (Klinkenberg effect), the local tangential permeability k_t in a planar pore is

$$k_t = \frac{(h - 2\Delta h)^2}{4}\left(\frac{1}{3} + \frac{\beta}{h - 2\Delta h}\right) \tag{2}$$

Here h is the interplatelet distance, Δh is the thickness of the adsorbed layer of water, and β is a slipping parameter for the flow boundary condition. From molecular dynamics simulations (Botan et al. 2011), β value is fixed at 0.21 nm. The term (h - $2\Delta h$) represents the effective accessible pore size. Formally, this relationship holds for planar pores with an opening larger than the thickness of a few water layers (e.g., 10) and continuum mechanics is no longer valid in smaller pores, where the discreteness of water molecules should be considered. However, here we accept continuum mechanics considerations for pore openings larger than one water layer, i.e. 0.3 nm, and smaller pores are assumed to be impermeable.

Equation (2) is considered to be a fair approximation for oblate pores with high aspect ratios and the local permeability is used in a one-step self-consistent scheme similar to the one proposed by Cariou(2010). Although in the present work the mineral solid matrix is not spherical, but oblate with the aspect ratio $\gamma_s < 1$. In this case, a small variation of the aspect ratio can lead to an order of magnitude difference in the homogenized permeability (Fig. 3). The localization tensor in the case of oblate pores,

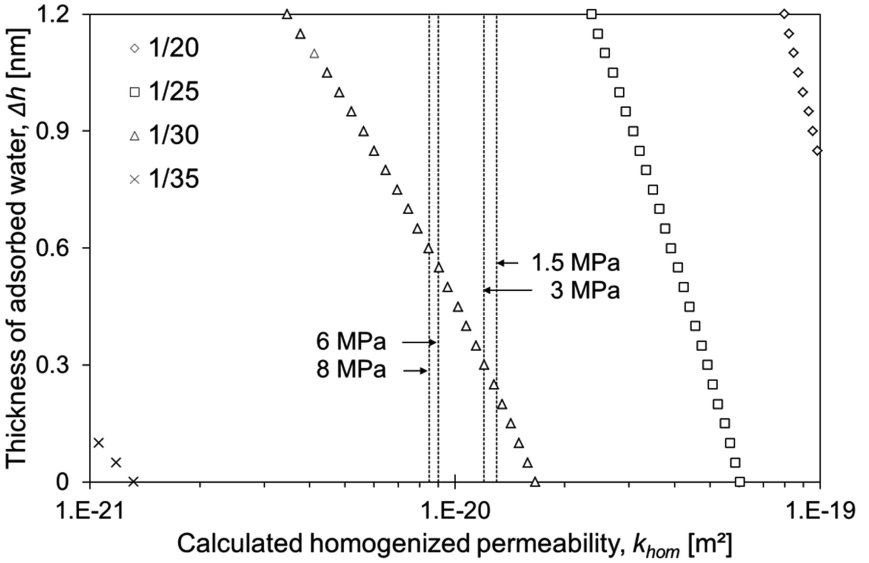

Fig. 3. Calculated homogenized permeability for different values of the thickness of the adsorbed water layer and different aspect ratio of the solid particles. The dashed vertical lines indicate the experimental results dependence on the differential fluid pressures.

or mineral inclusions, is calculated from equations provided by Giraud et al. (2015). This is a first order approach to derive shale properties, as a true homogenization scheme for shales should be two stepped: one step for the clay matrix and another one for the inert mineral inclusions.

The homogenization scheme is applied for different values of γ_s and Δh to investigate the influence of these parameters. Results are displayed in Fig. 3 and demonstrate the strong dependence on the solid aspect ratio, small variation of which can lead to an order of magnitude change in permeability. For a well-chosen solid aspect ratio, here 1/30, experimentally observed permeability decrease trend can be linked to the passage from one adsorbed water layer ($\Delta h \approx 0.3$ nm) to two layers ($\Delta h \approx 0.6$ nm). Adsorption of brine is then related to its pressure with a Toth (1971) adsorption isotherm:

$$\Delta h = \Delta h_m \frac{\left(p/p_{ref}\right)^t}{1 + \left(p/p_{ref}\right)^t} \tag{3}$$

where Δh_m is the maximum thickness of adsorbed water, chosen as a multiple of 0.3 nm, and p_{ref} and t are fitting parameters. Two examples of numerical simulations of sample permeability with this model are shown in Fig. 4, reproducing the decreasing permeability trend within the order of magnitude. Proper measurements of the adsorption parameters should be based on independent brine injection tests, while the intrinsic material permeability could be measured with an inert gas, providing further insight into the nature of complicated hydro-mechanical behavior of clays and shales.

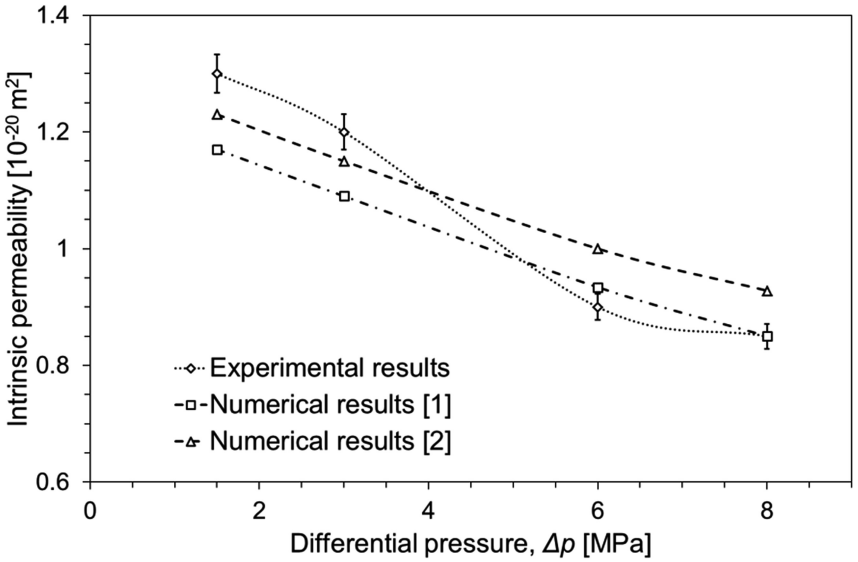

Fig. 4. Brine permeability evolution of remolded shale specimen with differential fluid pressure, experimental results (diamonds with error bars) and numerical simulations. Adsorption model parameters are Δh_m = 1.2 nm, p_{ref} = 13 MPa, and t = 3.5 in simulation [1] (squares), and Δh_m = 0.9 nm, p_{ref} = 12 MPa, and t = 4 in simulation [2] (triangles).

Conclusions

Flow measurements performed on a sample of remolded shale (Opalinus clay) show a significant decrease of brine permeability with increasing brine pressure. Influence of mechanical and thermal effects on this trend are negligible, while brine adsorption in the sample leading to a modification in the fluid accessible porosity has been considered as a possible option to explain the observed permeability decrease. Though numerical results are very sensitive to the hypothesis made for the pore structure (e.g., value of the solid particles aspect ratio) and the choice of parameters for the adsorption isotherm, they predict the decreasing permeability trend within the order of magnitude. For the better understanding of material behavior, permeability is suggested to be independently measured with an inert gas. Then, brine injection and flow tests could be used to determine the adsorption parameters and explain the complicated nature of hydro-mechanical behavior of clay-rich and shaley materials.

Acknowledgements. Opalinus clay cores were provided by Swisstopo in the framework of Mont Terri project, CS-C experiment. R. Makhnenko acknowledges the support from SCCER-SoE (Switzerland) grant KTI.2013.288 and Swiss Federal Office of Energy (SFOE) project CAPROCK #810008154.

References

ASTM D4767 (2011) Standard Test Method for Consolidated Undrained Triaxial Compression Test for Cohesive Soils

Bossart P (2012) Characteristics of the Opalinus Clay at Mont Terri. http://www.mont-terri.ch/internet/montterri/de/home/geology/key_characteristics.html

Botan A, Rotenberg B, Marry V, Turq P, Noetinger B (2011) Hydrodynamics in clay nanopores. J Phys Chem C 115(32):16109–16115

Cariou S (2010) Couplage hydro-mécanique et transfert dans l'argilite de Meuse/Haute-Marne: approches expérimentale et multi-échelle (Doctoral dissertation, Ecole des Ponts ParisTech)

Dormieux L, Kondo D, Ulm FJ (2006) Microporomechanics. Wiley, Chichester 327 p

Romero E, Senger R, Marschall P, Gomez R (2013) Air tests on low-permeability claystone formations. Experimental results and simulations. In: Laloui L, Ferrari A (eds) Multiphysical Testing of Soils and Shales., Springer Series in Geomechanics and Geoengineering, Springer, Heidelberg, pp 69–83

Giraud A, Sevostianov I, Chen F, Grgic D (2015) Effective thermal conductivity of oolitic rocks using the Maxwell homogenization method. Int J Rock Mech Mining Sci 80:379–387

Makhnenko RY, Labuz JF (2016) Elastic and inelastic deformation of fluid-saturated rock. Phil Trans R Soc A 374:20150422. doi:10.1098/rsta.2015.0422

Pearson FJ (2002) PC experiment: recipe for artificial pore water. Mont Terri Project, Technical Note 2002–17

Toth J (1971) State equations of the solid-gas interface layers. Acta Chim Acad Sci Hungar 69 (3):311–328

Weaver CE (1988) Clays, Muds, and Shales. Elsevier, Amsterdam, 819 p